Fugler, L., Clejan, S., & Bittman, R. (1985) *J. Biol. Chem. 260*, 4098-4100.
Gold, J. C., & Phillips, M. C. (1990) *Biochim. Biophys. Acta 1027*, 85-92.
Grönberg, L., & Slotte, J. P. (1990) *Biochemistry 29*, 3173-3178.
Guivisdalsky, P. N., & Bittman, R. (1989) *J. Org. Chem. 54*, 4637-4642.
Hammarström, S. (1971) *J. Lipid Res. 12*, 760-765.
Hui, S. W. (1988) in *Biology of Cholesterol* (Yeagle, P. L., Ed.) pp 1213-1231, CRC Press, Boca Raton, FL.
Hwang, J. S., & Cummins, H. Z. (1982) *J. Chem. Phys. 77*, 616-621.
Julina, R., Herzig, T., Bernet, B., & Vasella, A. (1986) *Helv. Chim. Acta 69*, 368-373.
Kan, C.-C., & Bittman, R. (1990) *J. Am. Chem. Soc. 112*, 884-887.
Kan, C.-C., Hajdu, J., & Bittman, R. (1991) *Biochim. Biophys. Acta 1066*, 95-101.
Lijana, R. C., McCracken, M. S., & Rudolph, C. J. (1986) *Biochim. Biophys. Acta 879*, 247-252.
Lund-Katz, S., Laboda, H. M., McLean, L. R., & Phillips, M. C. (1988) *Biochemistry 27*, 3416-3423.
McLean, L. R., & Phillips, M. C. (1981) *Biochemistry 20*, 2893-2900.
McLean, L. R., & Phillips, M. C. (1984) *Biochim. Biophys. Acta 776*, 21-26.
Pascher, I. (1976) *Biochim. Biophys. Acta 455*, 433-451.
Pascher, I., & Sundell, S. (1977) *Chem. Phys. Lipids 20*, 175-191.
Phillips, M. C., Johnson, W. J., & Rothblat, G. H. (1987) *Biochim. Biophys. Acta 906*, 223-276.
Ryu, E. K., & MacCoss, M. (1979) *J. Lipid Res. 20*, 561-563.
Sankaram, M., & Thompson, T. E. (1990) *Biochemistry 29*, 10670-10675.
Schmidt, R. R., & Kläger, R. (1982) *Angew. Chem. Int. Ed. Engl. 21*, 210-211.
Theunissen, J. J. H., Jackson, R. L., Kempen, H. J. M., & Demel, R. A. (1986) *Biochim. Biophys. Acta 860*, 66-74.
Thomas, P. D., & Poznansky, M. J. (1988) *Biochem. J. 251*, 55-61.
Van Blitterswijk, W. J., Van der Meer, B. W., & Hilkmann, H. (1987) *Biochemistry 26*, 1746-1756.
Van Dijck, P. W. M. (1979) *Biochim. Biophys. Acta 555*, 89-101.
Yeagle, P. L. (1988) in *Biology of Cholesterol* (Yeagle, P. L., Ed.) pp 121-145, CRC Press, Boca Raton, FL.
Yeagle, P. L., & Young, J. E. (1986) *J. Biol. Chem. 261*, 8175-8181.

Conformation and Disulfide Bond Formation of the Constant Fragment of an Immunoglobulin Light Chain: Effect of Truncation at the C-Terminal Region

Akihiro Ishiwata,[‡] Yasushi Kawata,[§] and Kozo Hamaguchi*
Department of Biology, Faculty of Science, Osaka University, Toyonaka, Osaka 560, Japan
Received February 5, 1991; Revised Manuscript Received April 16, 1991

ABSTRACT: Constant fragments with different carboxyl terminals, C_L(109–211), C_L(109–207), and C_L(109–200), were prepared by limited carboxypeptidase P or Y proteolysis of the constant fragment, C_L(109–214), of a type λ immunoglobulin light chain, and their conformations and stabilities, and formation of the disulfide bond from the reduced fragments, were studied. No change in conformation or stability was observed on removal of three residues from the C-terminal end. Removal of seven or more residues from the C-terminal end destabilized the C_L fragment. The rate of disulfide bond formation from reduced C_L(109–207) was about 7 times faster than that for C_L(109–214). These findings suggest that elongation of the polypeptide chain at least beyond the 207th residue is necessary for folding of the C_L fragment into a definite conformation.

Although many studies have been carried out on in vitro folding of proteins, the mechanism of folding in vivo is complicated and is not clearly understood. In addition to the problem of what factors are involved in the maturation and folding of nascent polypeptide chains in vivo, it is not clear whether the folding of proteins is initiated sequentially from the N-terminus (cotranslational folding) or after completion of the polypeptide chain (posttranslational folding) [see reviews: Jaenicke (1987), Tsou (1988), Wright et al. (1988), Baldwin (1989), and Fischer and Schmid (1990)]. Furthermore, it is unclear whether disulfide bonds are formed cotranslationally in vivo.

In our laboratory, the unfolding and refolding of the C_L[1] fragment of an immunoglobulin light chain have been studied in detail (Goto & Hamaguchi, 1982a,b, 1987; Tsunenaga et al., 1987; Goto et al., 1987; Kawata & Hamaguchi, 1991). In order to understand when folding of the C_L fragment is

[‡] Present address: Research Laboratories, Dainippon Pharmaceutical Co., Ltd., Suita, Osaka 564, Japan.
[§] Present address: Department of Chemistry, Faculty of Science, Kyoto University, Sakyo-ku, Kyoto 606, Japan.

[1] Abbreviations: CD, circular dichroism; C_L, constant fragment of immunoglobulin light chain; C_L(109–x), fragment corresponding to sequence 109–x of type λ light chain (Nag); CPase, carboxypeptidase; DTT, dithiothreitol; Gdn-HCl, guanidine hydrochloride; HPLC, high-performance liquid chromatography; SDS, sodium dodecyl sulfate; Tris, tris(hydroxymethyl)aminomethane.

0006-2960/91/0430-7766$02.50/0

completed during elongation of the polypeptide chain from the N-terminal, we prepared several C_L fragments whose C-terminal regions were truncated for different lengths and studied their conformations and stabilities.

We also studied the disulfide bond formation of a truncated C_L fragment. Previously, Goto and Hamaguchi (1981) studied the formation of the disulfide bond by oxidized glutathione from a reduced C_L fragment in the absence and presence of 8 M urea. It was found that the reaction of the reduced C_L fragment with oxidized glutathione was much slower whereas the yield of the C_L fragment bearing the disulfide bond was much higher in the absence of urea than in its presence. This is due to the fact that a pair of cysteinyl residues is buried in the interior of the reduced C_L fragment, being unable to react with glutathione in the absence of urea. Thus it is suggested that in vivo the disulfide bond is formed before completion of folding of the protein molecule. Indeed, the work of Bergman and Kuehl (1979) showed that the intrachain disulfide bonds of MPC 11 light chain in vivo are formed rapidly before completion of the primary structure.

The C_L fragment contains only one disulfide bond buried in the interior hydrophobic region of the molecule (Beale & Feinstein, 1976; Amzel & Poljak, 1979) and is thus very suitable for studying the correlation between disulfide bond formation and conformation. In the present study, we investigated the conformations and disulfide bond formation of truncated C_L fragments as a model of in vivo folding of nascent polypeptide chains.

Materials and Methods

Materials. CPase P was purchased from the Peptide Institute, Osaka, CPase Y from Oriental Yeast, and *Achromobacter lyticus* protease I from Wako Pure Chemicals. Gdn-HCl (specially purified grade) was purchased from Nacalai Tesque, and *trans*-4,5-dihydroxy-1,2-dithiane (oxidized DTT) was from Sigma. All other reagents were of the highest grade commercially available.

Preparation of C_L Fragment and C-Terminal-Truncated C_L Fragments. Immunoglobulin light chain Nag (type λ) was prepared from the urine of a multiple myeloma patient as described previously (Goto et al., 1979). C_L(109–214), in which Cys 213 was carboxamidomethylated, was obtained by papain digestion of Nag protein as described previously (Goto & Hamaguchi, 1979). This fragment has been used up to now in studies at our laboratory.

C_L(109–211) was obtained by CPase P digestion of C_L(109–214). C_L(109–214) was digested with CPase P in 50 mM sodium acetate buffer, pH 4.0, at 37 °C for 4.5 h at a substrate-to-enzyme ratio of 160:1 (mol/mol). The digestion product was subjected to gel filtration at 4 °C on a Sephadex G-75 column (3.6 × 114 cm) equilibrated with 10 mM Tris-HCl buffer, pH 8.6. Almost all the C_L fragments were eluted at the position corresponding to the undigested protein. This fraction was subjected to ion-exchange chromatography on a DEAE-cellulose column (2.0 × 40 cm). Two peaks were eluted with a linear gradient of 0–0.1 M KCl. Results of C-terminal amino acid analysis (see below) of these peaks showed that the first peak consisted of C_L(109–211) only. Fifteen milligrams of C_L(109–211) was obtained from 100 mg of C_L(109–214). C_L(109–211) was found not to contain other fragments on the basis of the amino acid composition and C-terminal analysis.

C_L(109–207) was obtained by CPase Y digestion of C_L(109–214). C_L(109–214) (200 mg) was digested with CPase Y in 50 mM sodium acetate buffer at pH 5.8 containing 1.3 M urea at 37 °C for 50 min at a substrate-to-enzyme ratio of 100:1 (mol/mol). The digestion was stopped by lowering the pH to 2. The digestion product was subjected to gel filtration on a Sephadex G-75 column (3.1 × 118 cm) equilibrated with 0.01 N HCl. The fractions of the main peak were collected, and the sample was subjected to ion-exchange chromatography on a DE-52 column (2.1 × 45 cm) equilibrated with 10 mM Tris-HCl buffer at pH 8.6. Two peaks were eluted with a linear gradient of 0–0.1 M KCl. The first peak was found to contain a mixture of C_L(109–207) and C_L(109–211) by C-terminal amino acid analysis. As will be described under Results, since C_L(109–207) is unfolded by 0.5 M Gdn-HCl but C_L(109–211) is not, C_L(109–207) was easily separated from C_L(109–211) by gel filtration on a Sephadex G-50 column (superfine, 2.8 × 90 cm) equilibrated with 10 mM Tris-HCl, pH 7.5, containing 0.5 M Gdn-HCl. Twelve milligrams of C_L(109–207) was obtained. C_L(109–207) was found not to contain other species on the basis of amino acid composition and the results of C-terminal analysis.

C_L(109–200) and C_L(109–196) were obtained by CPase Y digestion of C_L(109–214). C_L(109–214) (100 mg) was digested with CPase Y at a substrate-to-enzyme ratio of 100:1 (mol/mol) in 50 mM sodium acetate buffer at pH 5.8 containing 1.4 M urea for 2 h at 37 °C. The digestion product was subjected to gel filtration on a Sephadex G-75 column (3.6 × 114 cm) equilibrated with 10 mM Tris-HCl buffer. The peak eluting at the same position was C_L(109–214) had a wide shoulder at the faster side. The fractions corresponding to this shoulder were collected, and the sample was subjected to ion-exchange chromatography on a DE-52 column (2.1 × 45 cm) using a linear gradient of 0–0.1 M KCl. The results of C-terminal amino acid analysis showed that the unadsorbed fractions contained C_L(109–196) and that the peak eluted by 0.03 M KCl corresponded to C_L(109–200). Six milligrams of C_L(109–200) and 4 mg of C_L(109–196) were obtained. Determination of the amino acid composition and the C-terminal residue showed that the sample of C_L(109–200) contained 20% of other species differing in C-terminal length by a few residues and that the sample of C_L(109–196) contained 20% C_L(109–197).

Table I summarizes the amino acid sequences of the C-terminal-shortened C_L fragments used in the present experiments.

Table I: Sequences of C-Terminal-Truncated C_L Fragments (Type λ)[a]

	109 115	190	200	210 214
C_L(109-214)	SQPKAAP.....	.HKSYSCQVTHEGSTVEKTVAPTECS		
C_L(109-211)	SQPKAAP.....	.HKSYSCQVTHEGSTVEKTVAPT		
C_L(109-207)	SQPKAAP.....	.HKSYSCQVTHEGSTVEKT		
C_L(109-200)	SQPKAAP.....	.HKSYSCQVTHE		
C_L(109-196)	SQPKAAP.....	.HKSYSCQ		

[a] The N-terminal sequences were determined by Goto and Hamaguchi (1979). The C-terminal sequences were determined as described in the text.

C-Terminal Amino Acid Analysis. The C-terminal amino acid residues of the truncated C_L fragments were determined by hydrazinolysis (Schroeder, 1972). The amino acid compositions of the whole protein and the C-terminal peptides obtained by digestion with *A. lyticus* protease I were determined. A truncated C_L fragment was digested with the protease in 50 mM Tris-HCl buffer, pH 9.0, at 37 °C for 4 h by using a substrate-to-enzyme ratio of 400:1 (mol/mol). The peptides were analyzed and isolated by reverse-phase HPLC. The C-terminal peptide obtained was hydrolyzed with 6 N HCl in vacuo at 110 °C for 24 h. The amino acid compositions

were determined with an Irica amino acid analyzer, Model A-5500.

CD Measurement. CD measurements were carried out with a Jasco spectrophotometer, Model J-500A, equipped with a data processor. CD spectra were measured in 50 mM Tris-HCl buffer, pH 7.5, containing 0.15 M NaCl at 25 °C. The results were expressed as mean residue ellipticity, $[\theta]$, which is defined as $[\theta] - (100)(\theta_{obs})/(lc)$, where θ_{obs} is the observed ellipticity in degrees, l is the length of the light path, and c is the residue molar concentration. In the calculation of c, a value of 108 was used as the mean residue molecular weight. The protein concentration used was 0.2 mg/mL.

Fluorescence Measurement. Fluorescence measurements were carried out with a Hitachi fluorescence spectrophotometer, Model MPF-4, equippled with a spectral corrector. Tryptophyl fluorescence was measured by using 295-nm light for excitation in 50 mM Tris-HCl buffer, pH 7.5, containing 0.15 M NaCl at 25 °C. The protein concentration used was below 0.05 mg/mL. The fluorescence at 350 nm was linearly dependent on protein concentration at all the protein concentrations used (the optical density was 0.1 or less at 280 nm).

Thermal Unfolding. Thermal unfolding equilibria were measured in terms of the ellipticity at 218 nm in 10 mM sodium phosphate buffer at pH 7.5 containing 0.15 M NaCl. The temperature was increased continuously at a rate of 0.5 °C/min and monitored with a Sensortek Model BAT-12 thermometer. The reversibility was examined by measuring the ellipticity at 218 nm by lowering the temperature at a rate of 2 °C/min.

Kinetics of Unfolding and Refolding. The kinetics of unfolding and refolding of C_L(109–211) and C_L(109–207) were measured at 25 °C in 50 mM Tris-HCl buffer, pH 7.5, containing 0.15 M NaCl. Fast unfolding and refolding were measured on a Union Giken Stopper-flow spectrophotometer, Model RA-401, with fluorescence detection. Excitation was at 280 nm, and the emission above 330 nm was measured. The details of the apparatus have been described previously (Goto & Hamaguchi, 1982a). The unfolding was initiated by mixing a pH 7.5 protein solution with Gdn-HCl solution at a given concentration at pH 7.5 in a 1:1 ratio. The refolding was initiated by mixing a denatured protein solution in 1.8 M Gdn-HCl with a Gdn-HCl solution at a given concentration at pH 7.5 in a 1:5 ratio (Kawata & Hamaguchi, 1991).

Slow unfolding and refolding reactions were measured with the Hitachi fluorescence spectrophotometer. The excitation wavelength was 295 nm, and the emission was measure at 350 nm. The unfolding was initiated by manual mixing of a protein solution in 0 M Gdn-HCl at pH 7.5 with Gdn-HCl solution at a given concentration of Gdn-HCl, pH 7.5. The refolding was initiated by mixing manually a denatured protein solution in 1.8 M Gdn-HCl with Gdn-HCl solution at a given concentration. All the kinetic data were analyzed as described previously (Goto & Hamaguchi, 1982a).

Kinetics of Disulfide Formation. The disulfide bond of C_L(109–214) or C_L(109–207) was reduced with DTT in 6 M Gdn-HCl at pH 8.0 for 30 min. The reduced C_L fragment was obtained by removing the reagents by gel filtration on a Sephadex G-25 column equilibrated with 50 mM Tris-HCl buffer at pH 8.0 containing 0.15 M NaCl and 1 mM EDTA. The thiol–disulfide interchange reaction was started by adding oxidized DTT solution to the reduced C_L fragment solution. The final concentrations of oxidized DTT and protein were 50 mM and 0.04 mg/mL, respectively. The thiol–disulfide interchange reaction was quenched by adding a one-fifth volume of 0.5 M iodoacetic acid in 0.5 M Tris-HCl buffer at pH 8.1 containing 8 M Gdn-HCl to samples of the reaction mixture taken out at appropriate intervals. The quenched solution was kept for a few minutes at room temperature. During this quenching reaction, no disulfide exchange reaction occurred. The residual reagents were removed by gel filtration on a Sephadex G-25 column equilibrated with 25 mM NH_4HCO_3 and then lyophilized. The reoxidized C_L fragment was well separated from the reduced and alkylated C_L fragment by ion-exchange HPLC on a TSK-gel CM-25W column (4.6 × 250 mm) equilibrated with 10 mM sodium citrate buffer, pH 5.8, with a linear concentration gradient of NaCl. The amount of the reoxidized C_L fragment formed was expressed as the ratio of the peak area of the reoxidized C_L fragment to the sum of the peak area of the reoxidized C_L fragment and that of the reduced and alkylated C_L fragment.

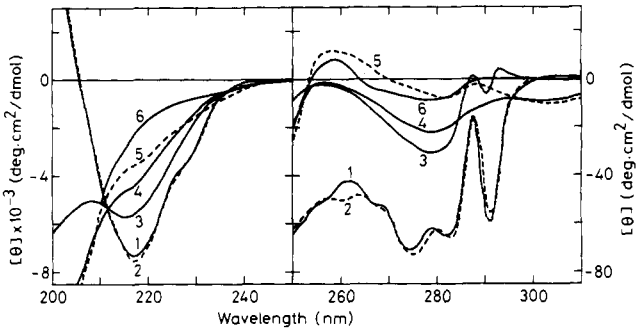

FIGURE 1: CD spectra of C-terminal-truncated C_L fragments at pH 7.5 and 25 °C. (1) C_L(109–214); (2) C_L(109–211); (3) C_L(109–207); (4) C_L(109–200); (5) C_L(109–196); (6) C_L(109–214) in 4 M Gdn-HCl.

All the thiol–disulfide interchange reactions were carried out by using buffers degassed and saturated with oxygen-free nitrogen under a nitrogen atmosphere.

Protein Concentration. Protein concentrations were determined spectrophotometrically. The absorption coefficients of the truncated C_L fragments used here were assumed to be the same as that of the intact C_L fragment, and a value of 16 800 M^{-1} cm^{-1} was used as the absorption coefficient at 280 nm (Karlsson et al., 1972).

Results

CD Spectra. Figure 1 shows the CD spectra of the C_L fragments truncated at the C-terminal region for different lengths at pH 7.5 and 25 °C. The CD spectrum of C_L(109–214) had a minimum at 218 nm, which is characteristic of the β-sheet conformation. The CD spectrum of C_L(109–211) was identical with that of C_L(109–214). The spectrum of C_L(109–207) also had a minimum of about 218 nm, but the negative ellipticity at 218 nm was smaller than that for C_L(109–214). The CD spectra of C_L(109–200) and C_L(109–196) were very similar to that of the thermally unfolded C_L(109–214) reported previously by Goto and Hamaguchi (1987).

Reduction of the intrachain disulfide bond did not unfold the C_L(109–214) molecule (Goto & Hamaguchi, 1979). In the case of C_L(109–207), however, unfolding occurred upon reduction of the disulfide bond.

Fluorescence Spectra. Figure 2 shows the fluorescence spectra of the various truncated C_L fragments. The fluorescence spectrum of C_L(109–211) was identical with that of C_L(109–214) and had a maximum at 320 nm. The fluorescence spectrum of C_L(109–207) had a broad maximum at around 340 nm and an intensity greater than that of C_L(109–211). The spectra of C_L(109–200) and C_L(109–196) were the same and had a maximum at 350 nm. The fluorescence intensity at the maximum for these fragments

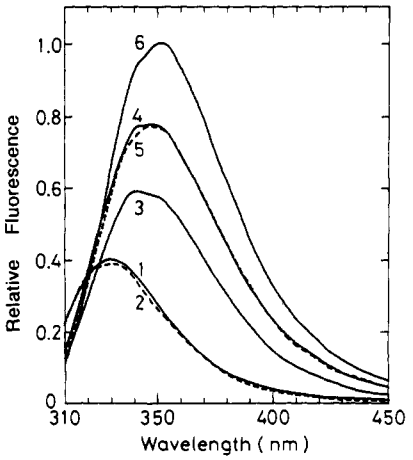

FIGURE 2: Fluorescence spectra of C-terminal-truncated C_L fragments at pH 7.5 and 25 °C. (1) C_L(109–214); (2) C_L(109–211); (3) C_L(109–207); (4) C_L(109–200); (5) C_L(109–196); (6) C_L(109–214) in 4 M Gdn-HCl.

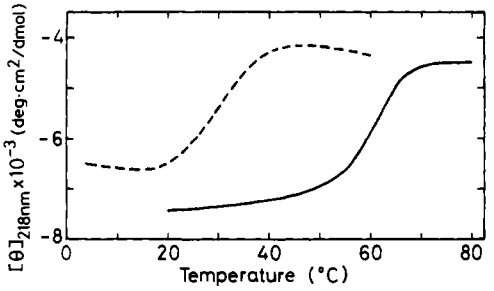

FIGURE 3: Thermal unfolding transitions of C_L(109–211) (solid line) and C_L(109–207) (broken line) in 0.01 M sodium phosphate buffer containing 0.15 M NaCl, pH 7.5. The transitions were measured in terms of the change in CD at 218 nm. The transition curve of C_L(109–214) was identical with that of C_L(109–211) within the experimental error.

was 0.75 relative to that for C_L(109–214) in 4 M Gdn-HCl. The fluorescence intensity at 350 nm for the unfolded C_L(109–214) in the absence of Gdn-HCl was estimated to be 0.75 relative to that in the presence of 4 M Gdn-HCl (Goto & Hamaguchi, 1982a). Thus the spectra of C_L(109–200) and C_L(109–196) indicated that these fragments are unfolded in the absence of Gdn-HCl.

Thermal Unfolding. Figure 3 shows the thermal unfolding curves for C_L(109–211) and C_L(109–207). The unfolding curve for C_L(109–211) was found to be the same as that for C_L(109–214), as measured by the ellipticity at 218 nm. The thermal unfolding curves were reversible. In contrast, the thermal stability of C_L(109–207) was much lower than that of C_L(109–211).

Unfolding by Gdn-HCl. We measured the unfolding of C_L(109–211) and C_L(109–207) by Gdn-HCl using changes in the ellipticity at 218 nm and fluorescence at 350 nm. In order to represent the two sets of experiments on the same scale, the transition curves were normalized by assuming that the ellipticity or fluorescence for the native and unfolded proteins which were observed before and after the transition zone, respectively, can be extrapolated linearly into the transition zone (Figure 4). The transition curve of C_L(109–211) was the same as that of C_L(109–214). The stability of C_L(109–207) against Gdn-HCl was much lower than that of C_L(109–211).

Kinetics of Unfolding and Refolding. Goto and Hamaguchi (1982a) reported that the kinetics of unfolding and refolding of C_L(109–214) can be described by two exponential terms:

$$F(t) - F(\infty) = F_1 \exp(-\lambda_1 t) + F_2 \exp(-\lambda_2 t) \quad (1)$$

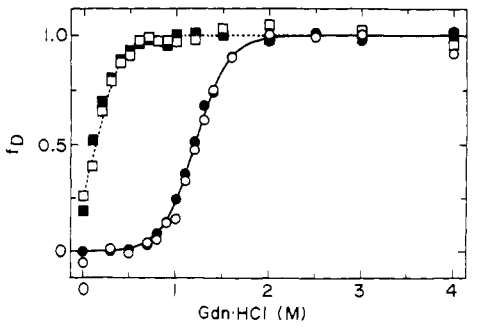

FIGURE 4: Unfolding transitions by Gdn-HCl of C_L(109–211) (○, ●) and C_L(109–207) (□, ■) at pH 7.5 and 25 °C. The unfolding transitions were measured in terms of the CD change at 218 nm (open symbols) and fluorescence intensity at 350 nm (solid symbols). The solid line indicates the theoretical curve of C_L(109–214) (Goto & Hamaguchi, 1987). The broken line represents the theoretical curve constructed on the basis of the parameters obtained by the Gdn-HCl binding method (Table III). The ordinate represents the unfolded protein fraction.

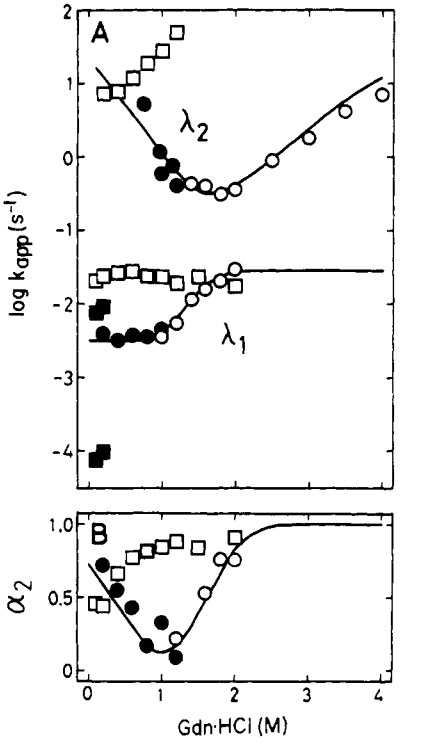

FIGURE 5: Dependence on Gdn-HCl concentration of the apparent rate constants (λ_1 and λ_2) and the relative amplitude (α_2) (B) of the fast phase for unfolding and refolding of C_L(109–211) (○, ●) and C_L(109–207) (□, ■) at pH 7.5 and 25 °C. The open symbols are obtained from unfolding kinetics and the solid symbols from refolding kinetics. The solid lines represent the values for C_L(109–214) cited from the previous paper (Goto & Hamaguchi, 1982).

where λ_1 and λ_2 are the apparent rate constants of the slow and fast phases, respectively, and F_1 and F_2 are the amplitudes of the respective phases. The amplitudes of the slow and fast phases relative of the total fluorescence change are described by α_1 and α_2, respectively, where $\alpha_1 + \alpha_2 = 1$. Figure 5 shows the kinetic parameters of the unfolding and refolding of C_L(109–211) and C_L(109–207) as a function of the concentration of Gdn-HCl. The kinetic parameters for C_L(109–211) were in good agreement with those for C_L(109–214) reported previously by Goto and Hamaguchi (1982a). The kinetic parameters for C_L(109–207) were greatly different from those for C_L(109–211). Although the apparent unfolding rate constant of the fast phase for C_L(109–207) was increased from 0.2 to 1.2 M Gdn-HCl, the apparent unfolding rate constant

Table II: Transition Midpoints and Thermodynamic Parameters of Thermal Unfolding of C_L Fragments with Different Carboxyl Terminals at pH 7.5

	T_m[a] (°C)	ΔH at T_m (kcal/mol)	ΔS at T_m (eu)	ΔG_D(25 °C) (kcal/mol)
C_L(109–214)	60.4 ± 0.1	66.9 ● 0.4	201 ± 1	3.5
C_L(109–211)	60.5 ± 0.1	67.1 ± 1.4	201 ± 4	3.6
C_L(109–207)	31.0 ± 0.3	36.6 ± 0.2	120 ± 1	0.5

[a] T_m is the temperature at the midpoint of the unfolding transition.

of the slow phase was almost constant.

Rate and Disulfide Bond Formation. C_L(109–214) and C_L(109–207) have only one disulfide bond each between Cys 136 and Cys 195. We measured the rate of disulfide bond formation from the reduced C_L(109–214) and C_L(109–207) fragments using oxidized DTT. Use of oxidized DTT simplifies the analysis of the reaction kinetics because no mixed disulfide is accumulated. Reduction of the disulfide bond unfolded the C_L(109–207) fragment but not the C_L(109–214) fragment. During the reaction, no appreciable intermolecular disulfide bond was formed for C_L(109–214) and C_L(109–207) judging from SDS–polyacrylamide gel electrophoresis (data not shown).

Figure 6 shows the time course of the formation of the disulfide bond for C_L(109–214) and C_L(109–207). The time course was approximated by pseudo-first-order kinetics, and the apparent rate constants of the disulfide bond formation of C_L(109–214) and C_L(109–207) in water were estimated to be 4.7×10^{-6} s^{-1} and 32×10^{-6} s^{-1}, respectively.

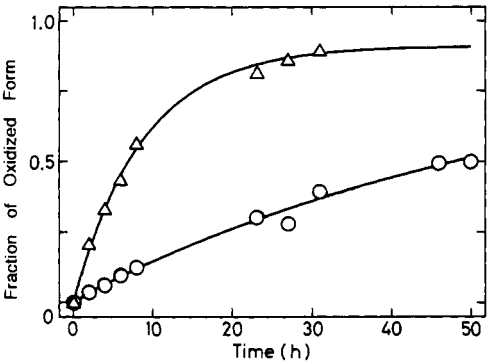

FIGURE 6: Kinetics of the formation of the intrachain disulfide bond of C_L(109–214) (○) and C_L(109–207) (△) at pH 8.0 and 25 °C. The solid lines were obtained by assuming pseudo-first-order kinetics. The apparent rate constants and the fractions of oxidized forms are as follows: 4.7×10^{-6} s^{-1} and 0.90 for C_L(109–214); 32×10^{-6} s^{-1} and 0.91 for C_L(109–207), respectively.

Discussion

Stability of Truncated C_L Fragments. The conformation and stability of C_L(109–211) were the same as those of C_L(109–214). However, the stability of C_L(109–207) against heat and Gdn-HCl was much lower than that of C_L(109–214). We analyzed the thermal transition curves of C_L(109–214) and C_L(109–211) assuming a two-state transition, N(native) $\rightleftharpoons$ D(unfolded), and the equilibrium constant of unfolding (K_D = [D]/[N]) was determined by using the equation $K_D = f_D/(1 - f_D)$, where f_D is the fraction of the unfolded molecule at each temperature. The enthalpy change (ΔH) at T_m was determined from the van't Hoff plot. At a given temperature (T), $\Delta H(T)$, $\Delta S(T)$, and $\Delta G(T)$ can be obtained by using the equations:

$$\Delta H(T) = \Delta H(T_m) + \Delta C_p(T - T_m) \quad (2)$$

$$\Delta S(T) = \Delta S(T_m) + \Delta C_p \ln (TT_m) \quad (3)$$

$$\Delta G(T) = \Delta H(T_m) - T\Delta S(T_m) + \Delta C_p[T - T_m - T \ln (T/T_m)] \quad (4)$$

In these calculations, a value of 1.8 kcal deg^{-1} mol^{-1} obtained for C_L(109–214) (Okajima et al., 1990) was also assumed for the change in heat capacity (ΔC_p) of C_L(109–211) and C_L(109–207). The thermodynamic parameters for the thermal unfolding of C_L(109–214), C_L(109–211), and C_L(109–207) are shown in Table II. As can be seen, truncation of three residues in the C-terminal region did not change the thermal stability, but truncation of seven residues resulted in marked destabilization of the molecule. Truncation of 14 residues or more unfolded the molecule completely (see Figure 1).

The unfolding curves produced with Gdn-HCl (Figure 4) were also analyzed by assuming a two-state approximation, and the free energy change of unfolding in the absence of Gdn-HCl, $\Delta G_D^{H_2O}$, was estimated according to two methods of extrapolation, a linear extrapolation method and a method based on the Gdn-HCl binding model [see Pace et al. (1989)]. Table III summarizes the values of $\Delta G_D^{H_2O}$ obtained for C_L(109–214), C_L(109–211), and C_L(109–207). It is shown that although the stability of C_L(109–211) is the same as that of C_L(109–214), the stability is greatly decreased on truncation of seven residues at the C-terminal end. The values of $\Delta G_D^{H_2O}$ obtained by the denaturant binding model were always larger than the respective values obtained by linear extrapolation. The values of ΔG_D (25 °C) obtained by analysis of the thermal unfolding curves (Table II) were near the values of $\Delta G_D^{H_2O}$ obtained by linear extrapolation rather than the corresponding values obtained by the denaturant binding model.

As reported by Goto and Hamaguchi (1982a), the unfolding and refolding kinetics of C_L(109–214) are expressed by eq 1 and can be explained on the basis of the mechanism:

$$U_1 \underset{k_{21}}{\overset{k_{12}}{\rightleftharpoons}} U_2 \underset{k_{32}}{\overset{k_{23}}{\rightleftharpoons}} N$$

where N is the native protein, U_1 and U_2 are the slow-folding and fast-folding species, respectively, of the unfolded protein, and k_{12}, k_{21}, k_{23}, and k_{32} are the rate constants of the respective processes. The kinetics of unfolding and refolding of C_L(109–207) are expressed by eq 1, and this suggests that the unfolding and refolding kinetics of c_L(109–207) can also be explained in terms of the above mechanism.

Table III: Transition Midpoints and Free Energy Changes of Unfolding of C_L Fragments with Different Carboxyl Terminals by Gdn-HCl at pH 7.5 and 25 °C

		denaturant binding model[b]		linear extrapolation[c]	
	C_m[a] (M)	$\Delta G_D^{H_2O}$ (kcal/mol)	Δn	$\Delta G_D^{H_2O}$ (kcal/mol)	m (kcal mol^{-1} M^{-1})
C_L(109–214)	1.2	5.7 ± 0.1	29.5 ± 0.3	4.1 ± 0.1	3.5 ± 0.1
C_L(109–211)	1.2	6.0 ± 0.2	30.7 ± 0.9	4.3 ± 0.1	3.5 ± 0.1
C_L(109–207)	0.1	0.6 ± 0.1	22.1 ± 1.0	0.6 ± 0.1	4.4 ± 0.3

[a] C_m is the concentration of Gdn-HCl at the midpoint of the unfolding transition. [b] The equation proposed by Tanford (1970), $\Delta G_D = \Delta G_D^{H_2O} - \Delta nRT \ln (1 + ka_\pm)$, was used, where Δn is the difference in the number of binding sites between the unfolded and folded states, k is the average binding constant of the sites, and $a_\pm$ is the mean ion activity of Gdn-HCl. We used a value of 0.6 M^{-1} for k (Pace et al., 1989). [c] The equation $\Delta G_D = \Delta G_D^{H_2O} - m$[Gdn-HCl] was used (Pace et al., 1989).

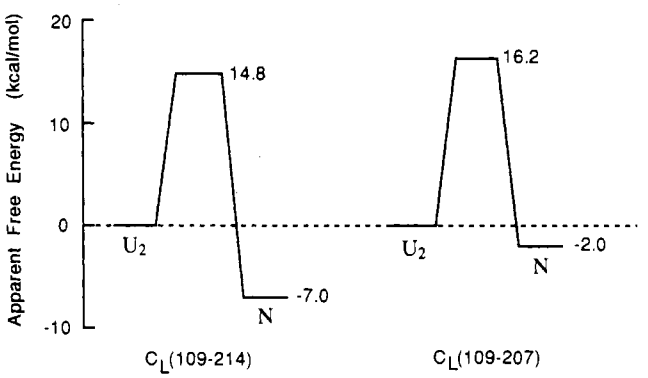

FIGURE 7: Free energy profiles for the unfolding and refolding of C_L(109–214) and C_L(109–207) at pH 7.5 and 25 °C. N and U_2 represent the folded and unfolded states, respectively. The profiles were constructed by setting the unfolded states of C_L(109–214) and C_L(109–207) at the same energy level.

The apparent equilibrium constant of unfolding (K_{app}) is expressed by the equation

$$K_{app} = \frac{[U_1] + [U_2]}{[N]} = \left(\frac{k_{21}}{k_{12}} + 1\right)\frac{k_{32}}{k_{23}} \quad (5)$$

We assumed that the value of k_{21}/k_{12} for C_L(109–207) is the same (10) as that for C_L(109–214), since the unfolded states, U_1 and U_2, for C_L(109–207) are the same as those for C_L-(109–214). This was also suggested by the fact that the observed values of λ_1 for C_L(109–207) are in agreement with those for C_L(109–214) above 2 M Gdn-HCl. Since $\lambda_1 = k_{23} + k_{32}$, we can estimate the values of k_{23} and k_{32} at various concentrations of Gdn-HCl. By extrapolation of these values to 0 M Gdn-HCl, the values of k_{23} and k_{32} in water were estimated to be 8.3 s^{-1} and 0.27 s^{-1}, respectively.

The activation free energy is calculated by using the equation

$$G^* = -RT \ln (kh/K_BT) \quad (6)$$

where k is the rate constant, h is Planck's constant, k_B is Boltzmann's constant, T is the temperature in kelvin, and R is the gas constant. Figure 7 shows the free energy profiles for C_L(109–207) and C_L(109–214) constructed by setting the unfolded states for both proteins at the same energy level. The difference in the activation free energy of unfolding between these proteins is estimated to be 3.6 kcal/mol, and the difference in the activation free energy of refolding is estimated to be 1.4 kcal/mol. This indicates that the instability of C_L(109–207) compared with C_L(109–214) is mostly explainable in terms of the increase in the unfolding rate rather than the decrease in the refolding rate.

Disulfide Bond Formation. The formation of the disulfide bond with oxidized DTT from the reduced C_L(109–214) fragment was slower than that for the reduced C_L(109–207) fragment (Figure 6). The reduced C_L(109–214) fragment has the same conformation as the intact fragment, and the two SH groups are buried in the interior of the molecule (Goto & Hamaguchi, 1979). Therefore, in order for the two SH groups to react with oxidized DTT, the reduced C_L(109–214) molecule must open and the two SH groups are exposed to solvent. Thus the rate of disulfide bond formation is rate-limited by this opening process. On the other hand, the conformation of the reduced C_L(109–207) fragment is disordered and the two SH groups are exposed to solvent and can easily react with oxidized DTT to form the disulfide bond. Kawata and Hamaguchi (1991) found that the unfolded C_L fragment molecule in aqueous solution has a compact conformation. Thus the distance between the two SH groups is short and the disulfide bond is formed effectively.

Elongation of a polypeptide chain in vivo proceeds from the N- to the C-terminus. Although various factors are involved in in vivo folding (Fischer & Schmid, 1990), our observations described above suggest that the disulfide bond is formed before the complete folding of the C_L fragment. The work of Bergman and Kuehl (1979) has shown that the intrachain disulfide bonds of MPC 11 light chain are formed rapidly before completion of the primary structure.

REFERENCES

Amzel, L. M., & Poljak, R. J. (1979) *Annu. Rev. Biochem. 48*, 961–997.
Baldwin, R. L. (1989) *Trends Biochem. Sci. 14*, 291–294.
Beale, D., & Feinstein, A. (1976) *Q. Rev. Biophys. 9*, 135–180.
Bergman, L. W., & Kuehl, W. M. (1979) *J. Biol. Chem. 254*, 8869–8876.
Fischer, G., & Schmid, F. X. (1990) *Biochemistry 29*, 2205–2212.
Goto, Y., & Hamaguchi, K. (1979) *J. Biochem. (Tokyo) 86*, 1433–1441.
Goto, Y., & Hamaguchi, K. (1981) *J. Mol. Biol. 146*, 321–340.
Goto, Y., & Hamaguchi, K. (1981a) *J. Mol. Biol. 156*, 891–910.
Goto, Y., & Hamaguchi, K. (1981b) *J. Mol. Biol. 156*, 911–926.
Goto, Y., & Hamaguchi, K. (1987) *Biochemistry 26*, 1879–1880.
Goto, Y., Azuma T., & Hamaguchi, K. (1979) *J. Biochem. (Tokyo) 85*, 1427–1438.
Jaenicke, R. (1987) *Prog. Biophys. Mol. Biol. 49*, 117–237.
Karlsson, F. A., Peterson, P. A., & Berggaord, I. (1972) *J. Biol. Chem. 247*, 1065–1073.
Kawata, Y., & Hamaguchi, K. (1991) *Biochemistry 30*, 4367–4373.
Okajima, T., Kawata, Y., & Hamaguchi, K. (1990) *Biochemistry 29*, 9168–9175.
Pace, C. N., Shirley, B. A., & Thomson, J. A. (1989) *Protein Structure, A Practical Approach* (Creighton, T. E., Ed.) pp 311–330, IRL Press, Oxford.
Schroeder, W. A. (1972) *Methods Enzymol. 25*, 138–143.
Tanford, C. (1970) *Adv. Protein Chem. 24*, 1–95.
Tsou, C.-L. (1988) *Biochemistry 27*, 1809–1812.
Tunenaga, M., Goto, Y., Kawata, Y., & Hamaguchi, K. (1987) *Biochemistry 26*, 6044–6051.
Wright, P. E., Dyson, H. J., & Lerner, R. A. (1988) *Biochemistry 27*, 7167–7175.